# A CONICAL BEAM SHIP ARRAY ANTENNA WITH INFINITELY VARIABLE CONTROL OF THE ELEVATION ANGLE

H. Forster, H.H. Mattes, A. Schrott
Deutsche Forschungs- und Versuchsanstalt für Luft- und Raumfahrt E.V. (DFVLR)
Institut für Flugfunk und Mikrowellen
8031 Oberpfaffenhofen, Germany

Studies on a ship terminal for a maritime satellite system [1, 2] have shown that a shipboard antenna with a 6 - 8 dB gain would have an optimum in costs. Therefore the DFVLR - Institut für Flugfunk und Mikrowellen decided to design an experimental shipboard antenna system meeting these datas. The first model of the antenna system was tested by the ESRO-Balloon-Simulation-Experiment during Sept./Oct. 1973 in the English Channel.

This system employs as radiator a conical beam antenna of vertical axis in the L-band (1535 to 1645 MHz) (figure 1). The angle of the cone is continuously variable by means of a triplate phase shifter especially developed for this system.

Radiator and phase shifter are mounted on a simple stabilized platform by means of which the radiation pattern of the antenna is held always in its normal position independent upon ship motions. The communication quality between ship and satellite therefore remains excellent also with strong rolling small ships. A further advantage is the independence of the satellite link on the ship's heading because of the fact, that the conical beam covers all 360 degrees of azimuth at the adjusted elevation angle.

As radiator a stacked cross-dipole antenna with ten elements is used (figure 2). Each element is designed to a medium frequency of 1590 MHz and covers the band 1535 - 1645 MHz. The ten radiator plates are made in stripline technique. They contain the radiating cross-dipoles and the integrated feeding networks generating the phase quadratures which are necessary to make a right hand circular polarized signal in the direction of the axis. Each element is fed by a separate coaxial cable. The ten feeders go down along the middle axis of the ten elements to the corresponding connectors of the phase shifter. The optimal distances between the radiating elements i and i + 1 (i = 1 - 9) are 0.45 wavelengths. The ten elements are mounted in a radom of fiberglass with 2 - 3 mm wall thickness and of cylindrical shape (diameter 115 mm, height incl. base 1042 mm). In a lower conical part of the radom the diameter increases to 352 mm forming a base which contains the phase shifter.

The radiation characteristic of the antenna was numerically determined in steps of five degrees of the elevation angle of the conical beam making use of the integral equation method. The mutual couplings of the elements also were considered. For the solution of the electromagnetic boundary problem the electrical field integral equation by Richmond [3] for straight thin wires was used.

$$-4\pi j\omega\varepsilon\vec{z} \cdot \vec{E}^{inc}(z) =$$

$$= \int_L I(z') \exp(-jkr)\, r^{-5} \cdot$$

$$\cdot \left[(1+jkr)(2r^2-3a^2) + k^2a^2r^2\right] dz'$$

$$r = \sqrt{(z-z')^2 + a^2}\,.$$

The geometrical relationships are represented in figure 3.

The numerical solution of this EFIE was carried out using the method of moments [4]. The unknown function is approximated by a series in a set of expansion functions with unknown coefficients. Multiplication of the integral equation by a set of testing functions results in a system of N linear equations in the unknown expansion coefficients. Written in matrix form the EFIE is transformed into

$$[Z_{ij}][\vec{I}_i] = [\vec{n} \times \vec{E}_i^{inc}]\,.$$

The mathematical model for the calculations of the radiation characteristics of the conical beam antenna is represented in figure 5. For convenience an already existing computer program was used which was developed for the solution of electromagnetic boundary problems of bodies with arbitrary shape excited by an incident field. This program bases on the wire-grid modelling technique suggested by Richmond. For each segment (max. 700 segments) of the wires the current is assumed to be constant (pulse functions as expansion functions) and the boundary conditions are enforced at the centres of each segment (point matching).

The measurements of the antenna patterns were carried out on antenna test range 2 of the Institut für Flugfunk und Mikrowellen of the DFVLR.

The calculated radiation patterns of the conical beam antenna for the orthogonal polarizations $E_\phi$ and $E_\theta$ are represented in figure 7 for one elevation angle of the conical beam.

Fig. 4 shows five calculated conical beam patterns with different beam elevation angles. The 6°-elevation pattern shows the minimum directivity (7.3 dB relative to the isotropic radiator). This results mainly from polarization loss due to the nearly linear polarization of the antenna radiation in this direction. The array

elements were matched at an array current distribution corresponding to the 6°-elevation characteristic. The gain losses due to mismatch of the radiator elements at higher beam elevation angles are tolerable, because the absolute directivity increases with the elevation. Measurements of the antenna patterns show satisfactory correspondence with the calculated diagrams.

The triplate phase shifter serves for adjusting the elevation angle of the conical beam. Ten outputs feed the lines to the ten radiating elements by radio frequency energy. The phase is controlled according to the elevation angle wanted. For a disk shaped pattern all radiating elements have equal phases. When the phase angles increase the cone angle 2 θ decreases. This is equivalent to higher elevation angles of radiation. The beam elevation angle is infinitely variable, therefore always the maximum gain of the lobes can be used.

The mechanical multiple phase shifter is composed of ten lines of variable length (trombones). Figure 6 shows the antenna feeding principle. The sine of the antenna beam elevation angle $\psi$ and the turning angle $\alpha$ of the phase shifter rotor are strict proportional:

$$\sin \psi = 2 \sqrt{\varepsilon}\, f(r_n, r_{n+1}, \omega) \cdot \frac{r_{n+1} - r_n}{d_n} \alpha \; ; \qquad n = 1 \ldots 9$$

- $\varepsilon$ permittivity of trombone dielectric
- $f$ corrective factor ($f \approx 1$)
- $r_n$ distance between turning axis and n-th trombone
- $d_n$ distance between n-th and (n+1)-th radiating element
- $\omega$ frequency.

The corrective factor $f \approx 1$ increases slightly with the curvature of the trombones. This effect was examinated experimentally. It is almost negligible.

The construction principle of the phase shifter is shown in figure 10. The rotor is driven by a servomotor and remote controlled. Rotor and stator are pressed together with a force of 350 N. The life of the sliding contracts is sufficient for many years because in typical applications the rotor is turned only once a day. Figure 8 shows the actual design of the ten channel phase shifter. All four platines consist of Cu-plated 1.6 mm PTFE-fiberglass. The rotor diameter is 280 mm. The maximum possible rotor turning angle of 115° induces variations of the electrical lengths of the outer and inner trombone of 1650° and 300° respectively, at a center frequency of 1.6 GHz. The characteristic impedance of all lines is 50 Ohms. The measured absolute mean phase errors of the prototype of the phase shifter are in all channels about 5°.

The stabilized pedestal (figure 9) supporting the radiator with radom and the phase shifter has two horizontal axes which are in parallel to the ship's pitch and roll axes. Two servomotors compensate the pitch and roll movements of the ship. The stabilization accuracy is ± 3°. Thereby the antenna radiation pattern is independent on the short term motions.

The pedestal is mounted on the mast or an other high place of the ship and is manufactured seawaterproof.

Swinging ranges are ± 25° for the pitch axis and ± 45° for the roll axis. Each axis is fitted with end switches and elastical limit stops and can be locked in zero position.

The masses are balanced so far that the center of gravity of movable parts lies a little below the axis. The wind forces are compensated only partially.

As a reference for controlling the pitch and roll servomotors a vertical gyro system is used to maintain the antenna axis in the vertical direction. The system has been mounted near the ship's center of mass to minimize the acceleration error. The signals indicating pitch and roll angles are related to the coordinate system of the ship.

All functions of the conical beam antenna system are controlled by a plug in unit which contains the following devices:

Power supply, regulators, power amplifiers, phase shifter control, control switches and indicating units.

The ac signals supplied by the gyro system are converted to dc signals. The amplitude of the signals depends linearly on the roll and pitch angles. These signals are compared with signals from the sensors on the antenna pedestal axes. From the error signals and the signals of the tacho generator amplified signals are derived to drive the servomotors. The phase shifter control button allows to set the conical beam exactly on the desired direction. Figure 11 shows the complete system.

References:


[1] Siemens AG, Parametric study, Ship terminal of a maritime satellite system,Volume 1 and 2, November 1972, ESTEC-Contract No. 1648/72 EL.

[2] The Marconi Company Limited, A Parametric Study of shipterminals in a maritime satellite system,Volume 1 and 2, Nov. 1972, ESTEC-Contract No. 1649/72 EL.

[3] Richmond, J.H. (1966), A wire grid model for scattering by conducting bodies, IEEE Trans. on Antennas and Propagation, AP-14, 782-786.

[4] Harrington, R.F. (1968), Field computation by moment methods, The Macmillan Company, New York.

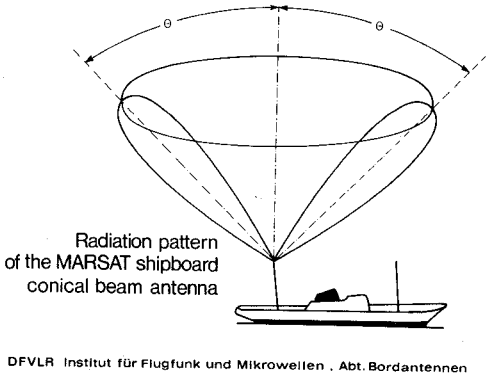


Figure 1. Conical beam pattern.

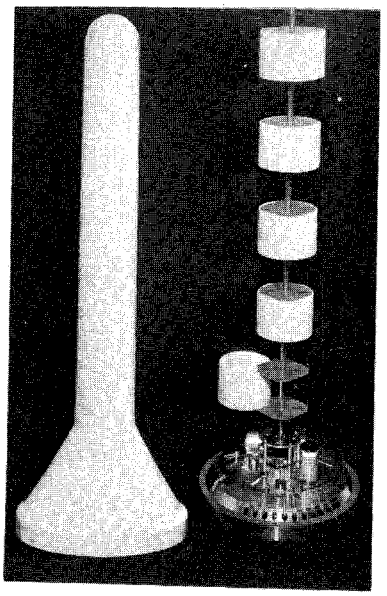

Figure 2. Radiator with radome.

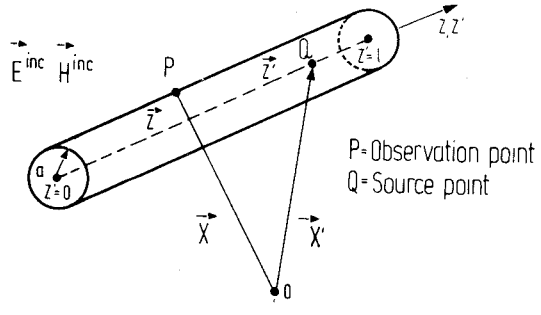


Figure 3. Geometry of a thin wire.

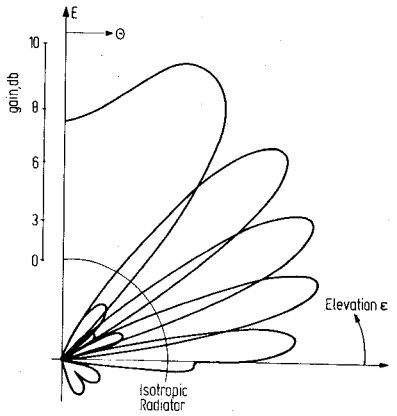


Figure 4. Calculated patterns for circular polarization.

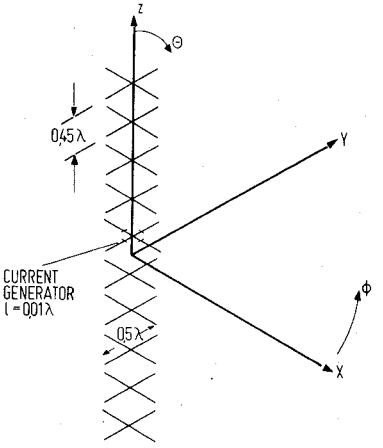


Figure 5. Antenna array.

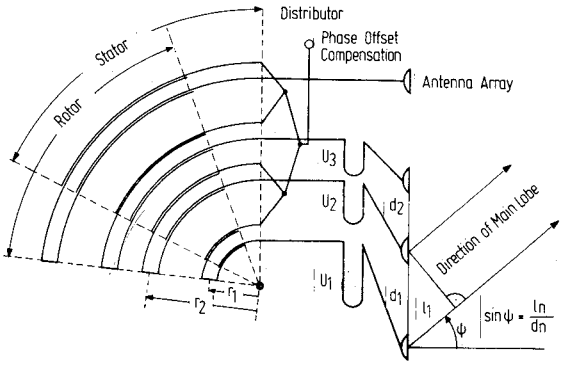


Figure 6. Principle of the multiple phase shifter.

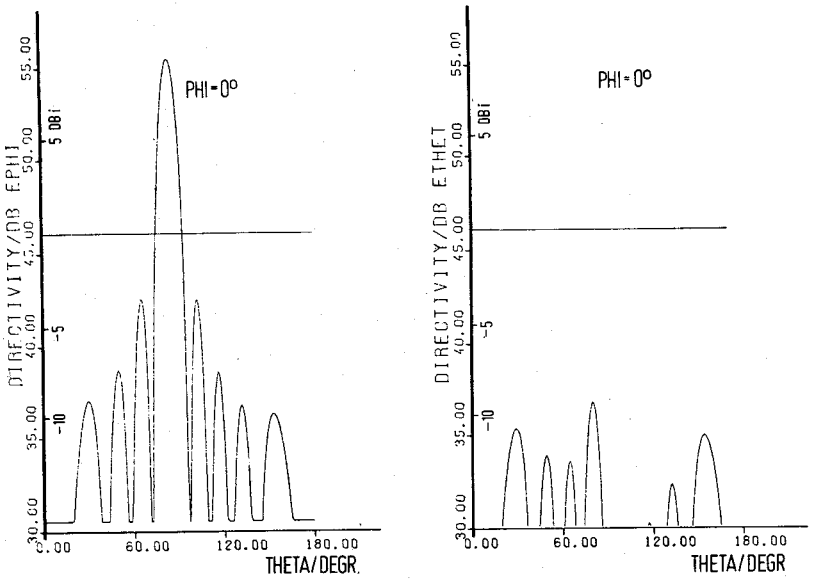


Figure 7. Calculated conical beam patterns for horizontal and vertical polarization.

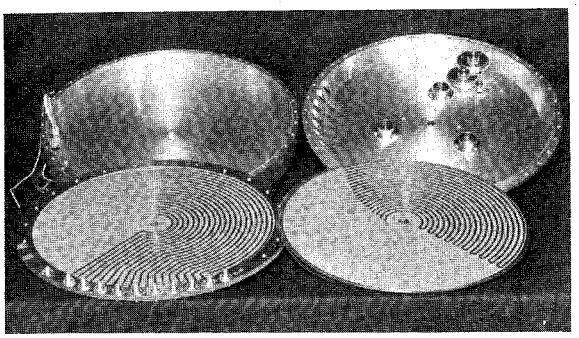

Figure 8. Phase shifter prototype.

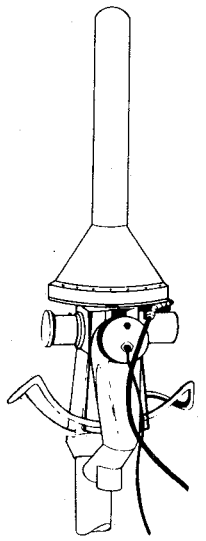

Figure 9. Stabilized pedestal.

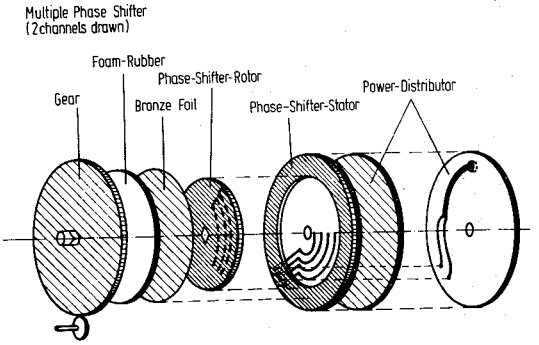


Figure 10. Construction principle of the phase shifter.

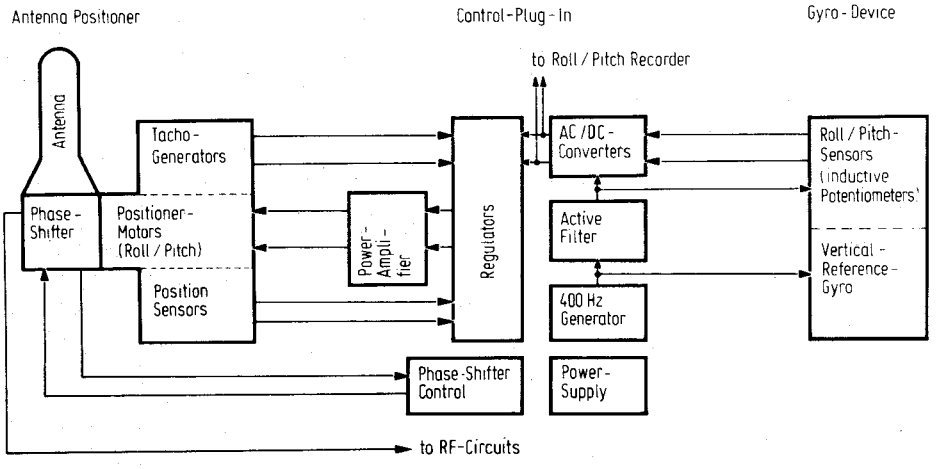


Figure 11. Block circuit of the conical beam antenna system.